LABORATORY INVESTIGATIONS

Anesthesiology
1997; 87:1381-93

The Effect of Halothane on the Recirculatory Pharmacokinetics of Physiologic Markers

Michael J. Avram, Ph.D., Tom C. Krejcie, M.D.,* Claus U. Niemann, M.D.,† Cheri Klein, B.A.,‡ W. Brooks Gentry, M.D.,§ Colin A. Shanks, M.D.,‖ Thomas K. Henthorn, M.D. **

Background: **The cardiovascular effects of halothane are well recognized, but little is known of how this affects drug distribution. The effect of halothane anesthesia on physiologic factors that affect drug disposition from the moment of injection was investigated.**

Methods: **The dispositions of markers of intravascular space and blood flow (indocyanine green), extracellular space and free water diffusion (inulin), and total body water and tissue perfusion (antipyrine) were determined in four purpose-bred coonhounds. The dogs were studied while awake and while anesthetized with 1%, 1.5%, and 2% halothane in a randomized order determined by a repeated measures Latin square experimental design. Marker dispositions were described by recirculatory pharmacokinetic models based on frequent early and less frequent later arterial blood samples. These models characterize the role of cardiac output and its distribution on drug disposition.**

Results: **Halothane caused a significant and dose-dependent decrease in cardiac output. The disposition of antipyrine was most profoundly affected by halothane anesthesia, which increased both nondistributive intercompartmental clearance and volume while decreasing fast and slow tissue clearances and elimination clearance in a halothane dose-dependent manner.**

Conclusions: **Halothane-induced changes in blood flow to the compartments of the antipyrine recirculatory model were not proportional to changes in cardiac output. Halothane anesthesia significantly increased (to more than double) the area under the drug concentration *versus* time curve due to an increase in the apparent peripheral blood flow not involved in drug distribution, despite a dose-dependent cardiac output decrease. Recirculatory pharmacokinetic models include the best aspects of traditional compartmental and physiologic pharmacokinetic models while offering advantages over both. (Key words: Anesthetics, volatile: halothane; influence on recirculatory pharmacokinetics in dogs. Blood flow and effect of halothane on drug distribution in dogs. Blood volume and effect of halothane on drug distribution in dogs. Heart: cardiac output; effect of halothane on drug distribution in dogs. Pharmacokinetics models: recirculatory; halothane anesthesia in dogs. Pharmacokinetics: distribution; halothane anesthesia in dogs.)**

This article is accompanied by an Editorial View. Please see: Wood M: Drug distribution — Less passive, more active? ANESTHESIOLOGY, 1997; 87:1274-6.

* Associate Professor of Anesthesiology.

† Research Fellow in Anesthesiology. Present address: Resident in Anesthesia, Department of Anesthesia (310), University of California at San Francisco, 521 Parnassus Avenue, San Francisco, California 94143-0648.

‡ Research Technician in Anesthesiology.

§ FAER Schering-Plough Research Fellow for 1992 and 1993. Present address: Assistant Professor, Department of Anesthesiology, University of Arkansas for Medical Science, 4301 West Markham, Slot 515, Little Rock, Arkansas 72205-7199.

‖ Professor of Anesthesiology.

Received from Northwestern University Medical School Department of Anesthesiology, Chicago, Illinois. Submitted for publication January 10, 1997. Accepted for publication July 28, 1997. Supported in part by National Institutes of Health grants GM43776, GM47502, and GM47819. Presented in part at the annual meeting of the American Society of Anesthesiologists, Washington, DC, October 9-13, 1993.

Address reprint requests to Dr. Avram: Northwestern University Medical School, Department of Anesthesiology, 303 E. Chicago Avenue, CH-W139, Chicago, Illinois 60611-3008. Address electronic mail to: mja190@nwu.edu

POTENT volatile anesthetics have profound systemic hemodynamic effects.[1] Studies of the effects of general anesthesia on drug disposition have focused largely on anesthetic-induced decreases in elimination clearance (Cl_E) due to decreased blood flow to eliminating organs (*e.g.*, the kidneys and liver) and decreased metabolism.[2] Few studies have examined systematically the effects of general anesthesia on drug distribution throughout the body.

The safe dose of an intravenously administered drug that has a rapid onset of effect and a low margin of safety, such as intravenous anesthetics, depends on its initial volume of distribution and early disposition, because sites of drug action are exposed to the high early drug concentrations in the minutes after drug administration.[3] To have a rational basis for dose selection, it

is important to characterize the initial disposition of a drug as accurately as possible. The three-compartment pharmacokinetic model fails to do this because it is based on infrequently collected blood samples beginning after the peak effect of a rapidly acting drug has begun to wane. In addition, the traditional model fails to account for the processes responsible for drug distribution and variability in the dose-response relation: mixing, flow, and diffusion.[4]

We developed a pharmacokinetic methodology that uses frequent early arterial blood sampling and a recirculatory pharmacokinetic model to describe the simultaneous disposition of markers with well-defined distribution from the moment of right atrial injection[5] (see appendix 1). These physiologic markers identify intravascular space, extracellular space, and total body water as well as intravascular mixing, blood flow, and free water diffusion. They serve not only as physiologic markers but also as prototypes or pharmacokinetic surrogates for other drugs.

Indocyanine green (ICG) binds to plasma proteins rapidly and completely, impeding its extravascular distribution. Thus it can be used to estimate blood volume based on back extrapolation of the postmixing monoexponential blood ICG concentration history.[6,7] Indicator (dye) dilution cardiac output (CO) can be estimated from the first-pass arterial blood ICG concentrations *versus* time relation.[8] Combined description of both the monoexponential blood ICG concentration history and the earlier mixing phase with a recirculatory pharmacokinetic model allows characterization of intravascular mixing by deriving estimates of not only blood volume and CO but also their systemic distribution (fig. 1).[9] Although ICG Cl_E can be used to estimate hepatic blood flow in some species,[10] its hepatic extraction ratio in the dog is less than 20%,[11] so its Cl_E should not change with halothane-induced decreases in hepatic blood flow.

The polysaccharide inulin distributes from intravascular space to interstitial fluid by free water diffusion through aqueous endothelial fenestrations.[12] Thus intercompartmental clearances (drug transport) to fast and slow tissue compartments are small.[5] Because little inulin exchanges with tissue space on a single pass, most blood flow is, in effect, nondistributive.[5] Therefore, most of CO in the recirculatory inulin model appears as fast and slow nondistributive pathways, which are nearly identical to the fast and slow peripheral intravascular circuits identified by ICG (fig. 1).[5] Inulin is a prototype for hydrophilic drugs, such as neuromuscular

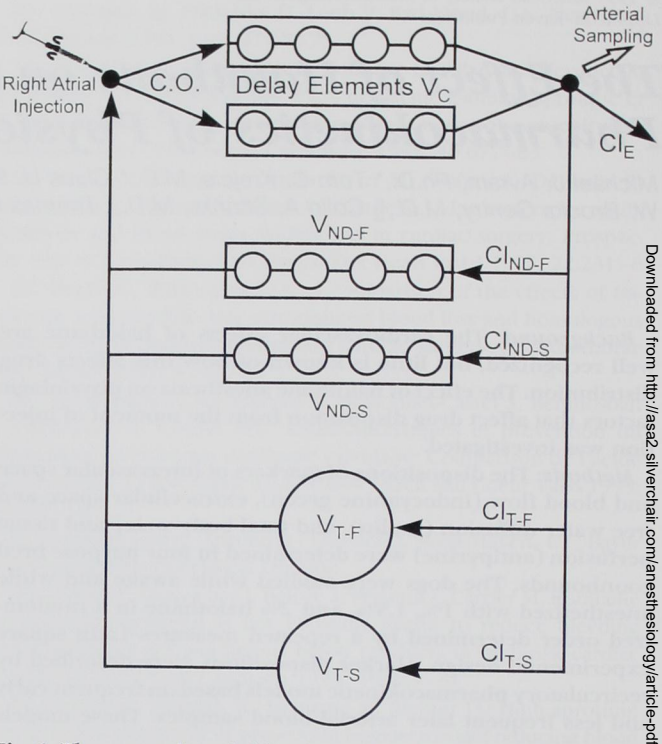

Fig. 1. The general model for the recirculatory pharmacokinetics of indocyanine green (ICG), inulin, and antipyrine. The central circulation of all three drugs receives all of cardiac output (CO) defined by the delay elements (V_C). The delay elements are represented generically by rectangles surrounding four compartments, although the actual number of compartments needed varied between 2 and 30 in any given delay. Beyond the central circulation, the CO distributes to many circulatory and tissue pathways which lump, based on their blood volume to blood flow ratios or tissue volume to distribution clearance ratios (MTTs), into fast (Cl_{ND-F}, V_{ND-F}) and slow (Cl_{ND-S}, V_{ND-S}) peripheral blood circuits (ICG) or nondistributive peripheral pathways (inulin and antipyrine) and fast (Cl_{T-F}, V_{T-F}) and slow (Cl_{T-S}, V_{T-S}) tissue volume groups.[5] Indocyanine green, which distributes only within the intravascular space, does not have fast and slow tissue volumes.[5] Antipyrine does not have an identifiable second nondistributive peripheral circuit. The elimination clearance (Cl_E) of all three markers are modeled from the arterial sampling site without being associated with any particular peripheral circuit.

blockers, that distribute to interstitial fluid by free water diffusion. Inulin's Cl_E is a measure of glomerular filtration rate, which is decreased by halothane anesthesia.[13]

Antipyrine is a marker of total body water,[14] including pulmonary extravascular water.[15] It distributes to a volume as large as total body water in a blood flow-dependent manner in many tissues and is thus a prototype for many lipophilic drugs,[16] including intravenous anesthetics. Unlike the intravenous anesthetics, antipyrine has no systemic cardiovascular effects that would affect

Table 1. Subject Characteristics and Global Pharmacokinetic Parameters

End-tidal Halothane Concentration	Weight (kg)	Hct* (%)	HR* (bpm)	MAP* (mmHg)	Cardiac Output*,† (L/min)	SVR (dyne·s·cm^{-5})	ICG V_{SS} (L/kg)	ICG Cl_E (ml·min^{-1}·kg^{-1})	Inulin V_{SS}‡ (L/kg)	Inulin Cl_E*,‡ (ml·min^{-1}·kg^{-1})	Antipyrine V_{SS}‡ (L/kg)	Antipyrine Cl_E*,‡ (ml·min^{-1}·kg^{-1})
0% (awake)	27.6	41.3	80	103	4.4	2,047	0.080	10.01	0.20	4.42	0.66	7.42
	(6.4)	(1.5)	(6)	(19)	(0.9)	(832)	(0.007)	(2.55)	(0.04)	(0.83)	(0.09)	(1.49)
1.0%	27.6	34.3§	88	79§	3.3	2,098	0.077	8.78	0.23	3.77§	0.68	2.92§
	(6.4)	(3.1)	(16)	(15)	(0.5)	(217)	(0.013)	(1.71)	(0.01)	(0.75)	(0.05)	(1.76)
1.5%	27.6	34.5§	99	64§	2.5§	2,059	0.082	9.42	0.25	3.73§	0.81	2.30§
	(6.4)	(3.0)	(9)	(8)	(0.4)	(363)	(0.015)	(2.80)	(0.05)	(1.03)	(0.11)	(0.27)
2.0%	27.6	31.6§	108§	60§	2.4§	2,229	0.080	8.30	0.24	2.35§	0.80	1.93§
	(6.4)	(3.2)	(8)	(7)	(0.7)	(453)	(0.011)	(2.39)	(0.02)	(1.16)	(0.16)	(0.23)

Values are mean (SD).

Hct = hematocrit; HR = heart rate; MAP = mean arterial pressure; SVR = systemic vascular resistance; V_{SS} = the sum of all compartmental volumes (the volume of distribution at steady-state); Cl_E = the elimination clearance.

* Significantly correlated with end-tidal halothane concentration ($P < 0.05$) as determined by Spearman rank order correlation.

† Determined by thermal dilution.

‡ Inulin and antipyrine V_{SS} and Cl_E are here presented on the basis of plasma rather than blood concentrations.

§ Significantly different from awake control ($P < 0.05$) as determined by Dunnett's test.

its own disposition. The recirculatory antipyrine pharmacokinetic model, like that of inulin, retains the fast and slow tissue distribution compartments of traditional three-compartment models while accurately predicting drug concentrations during early drug distribution, when many drugs produce their maximal effect.[17] In addition, it describes the role of CO and its distribution on lipophilic drug disposition. Antipyrine Cl_E depends on the hepatic microsomal mixed-function oxidase system[18] and is decreased even 48 h after halothane anesthesia.[19]

We used this new pharmacokinetic method to compare the physiologic factors affecting drug disposition in dogs when they were awake and when they were anesthetized with three levels of halothane anesthesia.

Materials and Methods

Experimental Protocol

The design of this pharmacokinetic study entailed 16 individual experiments. Four purpose-bred male coonhounds, weighing 18–31.5 kg (27.6 ± 6.4 kg, table 1), were studied on four occasions each in this study approved by our institutional animal care and use committee. Approximately 1 month before being studied, a Vascular-Access-Port catheter (Access Technologies, Skokie, IL) was placed into a femoral artery of each dog and secured to the muscle fascia of the upper hind leg to facilitate frequent percutaneous arterial blood sampling.[20] The dogs were allowed to recover from surgery for at least 2 weeks before being studied for the first time; the interval between subsequent studies was no less than 2 weeks.

All dogs were studied while awake (0% halothane, control) and while anesthetized with halothane at end-tidal concentrations of 1%, 1.5%, and 2%, which correspond to 1.2, 1.7, and 2.3 minimum alveolar concentration,[21,22] the order of which was randomized using a repeated measures Latin square experimental design. The dogs were trained to lie in the left lateral decubitus position for the awake study.

On the day of an awake study, the dog was brought to our laboratory and positioned. When it was determined that the dog was cooperative, the neck was prepped and the skin overlying the right external jugular vein was infiltrated liberally with 2% 2-chloroprocaine. Using a modified Seldinger technique, an 8-French percutaneous sheath introducer was inserted into the external jugular vein. If the insertion could not be accomplished in a timely and humane manner, the study was abandoned and rescheduled.

When the dogs were studied while anesthetized, anesthesia was induced with methohexital (10–15 mg/kg given intravenously) *via* a foreleg vein, the trachea was intubated with a 9-mm tracheal tube, and the animal was placed in the left lateral decubitus position. Mechanical ventilation was instituted at a tidal volume of

20–25 ml/kg at a rate sufficient to maintain end-tidal carbon dioxide tension at 30 ± 5 mmHg. Anesthesia was maintained with 1%, 1.5%, or 2% halothane in oxygen. End-tidal halothane concentrations were monitored with an Engstrom EMMA (Engstrom Medical AB, Bromma, Sweden) after its calibration with known standards. A heat and moisture exchanger was placed between the endotracheal tube and the EMMA in-line detector to minimize interference by water vapor.

For all studies, after an overnight fast during which the dog was allowed water *ad libitum*, the dog was brought to the laboratory and arterial access for blood sampling by roller pump or syringe was achieved by inserting a 20-gauge Huber needle percutaneously in the Vascular-Access-Port; this also allowed systemic arterial blood pressure to be monitored *via* a solid-state pressure transducer (Trantec; Baxter-Edwards, Irvine, CA). A flow-directed thermal dilution pulmonary artery catheter (Baxter-Edwards 93A-140-7F, with a 20-cm proximal port) was inserted through a sheath introducer in the right external jugular vein, positioned, and secured for determination of pulmonary arterial pressure and thermal dilution CO and to facilitate right atrial administration of the physiologic markers. The side arm of the sheath introducer was used for maintenance fluid administration and readministration of autologous blood. Hydration was maintained throughout the study by an infusion of 0.9% saline at a rate of 5–10 $ml \cdot kg^{-1} \cdot h^{-1}$ to maintain a constant pulmonary artery diastolic pressure (±2 mmHg). Once the study was well underway, a well-lubricated 7-French single-lumen, balloon-tipped catheter was inserted through the urethra into the bladder to facilitate urine ([^{14}C]-inulin) collection. All dogs, whether awake or anesthetized, easily tolerated this procedure.

One hundred fifty milliliters of whole blood was removed from the dog through the arterial catheter and anticoagulated with 1,000 U heparin. This blood was immediately replaced with 600 ml 0.9% saline solution administered intravenously for 30 min. During the first 10 min of the study (from time t = 0 min to t = 10 min), this autologous blood was reinfused intravenously to replace the blood obtained during the period of frequent blood sampling.

The study was not begun until the dog was hemodynamically stable. This was defined as less than 10% variation of CO and pulmonary and systemic arterial blood pressures during a 30-min period when measured every 15 min. The dogs were hemodynamically stable approximately 1 h after removal and saline replacement of the 150 ml blood.

At the onset of the study (time t = 0 min), ICG (Cardio-Green; Hynson, Westcott, and Dunning, Baltimore, MD), 5 mg in 1 ml of diluent, [^{14}C]-inulin (DuPont NEN, Boston, MA), 30 μCi in 1.5 ml of diluent, and antipyrine (Sigma Chemical Co., St. Louis, MO), 25 mg in 1 ml of diluent, were injected within 1 s through the proximal pulmonary artery catheter port. Arterial blood samples were collected every 0.05 min for the first minute and every 0.1 min for the next minute using a computer-controlled roller pump (Masterflex; Cole-Parmer, Chicago, IL) and chromatography fraction collector (model 203; Gilson, Middleton, WI). Subsequent arterial blood samples were drawn manually at 0.5-min intervals to 4 min, every 2 min to 20 min, every 10 min to 60 min, every 15 min to 120 min, and every 30 min to 360 min.

Analytical Methods

Plasma ICG concentrations of all samples obtained up to 20 min were measured on the study day using the high-performance liquid chromatography technique of Grasela *et al.*[23] as modified in our laboratory to provide sensitivity of 0.2 to 20.00 μg/ml with coefficients of variation of 5% or less.[8] Plasma ICG concentrations were converted to blood concentrations by multiplying them by one minus the hematocrit concentration because ICG does not partition into erythrocytes.

Plasma [^{14}C]-inulin concentrations of all samples were determined by liquid scintillation counting, using an external standard method for quench correction.[24] Counts that were less than three times the background count were considered to be less than the lower limit of detection. The coefficient of variation of the assay was less than 3%. Plasma inulin concentrations were converted to blood concentrations by multiplying them by one minus the hematocrit, because inulin does not partition into erythrocytes.

Plasma antipyrine concentrations were measured in all samples using a modification of a high-performance liquid chromatography technique developed in our laboratory.[5,17] The antipyrine method is linear from plasma concentrations of 0.10 to 10.00 μg/ml with coefficients of variation of 5% or less. Plasma antipyrine concentrations were converted to blood concentrations using an *in vivo* technique.[5]

Data Analysis

Arterial marker concentration *versus* time data before evidence of ICG recirculation (*i.e.*, first-pass data) were

weighted uniformly and fitted to the sum of two right-skewed gamma (Erlang) distribution functions using TableCurve 2D (version 3.0; Jandel Scientific, San Rafael, CA) on a Pentium-based PC (Gateway 2000, North Sioux City, SD).[25] Because neither ICG nor inulin distribute beyond the intravascular space before recirculation, they were modeled simultaneously to improve the confidence in the model parameters of the central (first-pass) circulation. Antipyrine has measurable tissue distribution during this time and was modeled independently.

In subsequent pharmacokinetic analysis, the descriptions of the central circulation were incorporated as parallel linear chains, or delay elements, into independent recirculatory models for the individual markers using SAAM II (SAAM Institute, Seattle, WA) implemented on a Pentium-based PC.[25,26] The first-pass data were excluded from further data fitting; the results of the Erlang model of the central circulation were placed as fixed parameters into the recirculatory model, thereby reducing the number of parameters to be optimized. The data were weighted in proportion to the reciprocal of the estimated variance for each datum, assuming all data have estimated fractional standard deviations of 0.5. Possible model misspecification was examined by testing for random scatter about the calculated values[27] using the two-tailed one-sample runs test, with $P < 0.05$, corrected for multiple applications of the runs test, as the criterion for rejection of the null hypothesis.[28]

The Pharmacokinetic Model

The pharmacokinetic modeling method was based on the approach described by Jacquez[29] for obtaining information from outflow concentration histories, the so-called inverse problem (fig. 1). Inulin and antipyrine distribution to extracellular fluid space and total body water space, respectively, were analyzed as the convolution of their intravascular behavior, determined by the pharmacokinetics of concomitantly administered ICG, and tissue distribution kinetics.[5]

The intravascular mixing model of ICG disposition has been modified from that which we described previously because of the improved descriptions of circulatory delays enabled by SAAM II.[9,5] The two lumped parallel pathways of the central circulation, described by the sum of two Erlang distribution functions, were incorporated into a full recirculatory model, including lumped parallel fast and slow peripheral circuits and Cl_E, using SAAM II. The antipyrine pulmonary tissue volume ($V_{T\text{-}P}$) is the difference between the antipyrine central volume (mean transit time $[MTT]_{antipyrine} \cdot CO$) and the central intravascular volume codetermined by ICG and inulin ($MTT_{ICG,inulin} \cdot CO$).

Peripheral drug distribution can be lumped into identifiable volumes and clearances: a fast nondistributive peripheral pathway ($V_{ND\text{-}F}$ and $Cl_{ND\text{-}F}$), a slow nondistributive peripheral pathway ($V_{ND\text{-}S}$ and $Cl_{ND\text{-}S}$), rapidly (fast) equilibrating tissues ($V_{T\text{-}F}$ and $Cl_{T\text{-}F}$), and slowly equilibrating tissues ($V_{T\text{-}S}$ and $Cl_{T\text{-}S}$). The fast and slow nondistributive peripheral pathways (delay elements) represent intravascular circuits in the ICG and inulin models; the single nondistributive peripheral pathway in the antipyrine model represents pathways with minimal apparent tissue distribution. In the inulin and antipyrine models, the parallel rapidly and slowly equilibrating tissues are the fast and slow compartments of traditional three-compartment pharmacokinetic models, respectively, and therefore the central circulation and nondistributive peripheral pathways are detailed representations of the ideal central volume of the three-compartment model.[9] Because of the direct correspondence between the recirculatory model and three-compartment models, Cl_E was modeled from the arterial (sampling) compartment to allow comparison of these results with previous ones.

The eight model variables determined from arterial blood ICG concentrations, the nine model variables determined from arterial blood antipyrine concentrations, and the 12 model variables determined from arterial blood inulin concentrations were determined to be both sensible and identifiable for our sampling schedule by the IDENT2 program of Jacquez and Perry.[30,5]

Statistical Analysis

The effect of the order of treatment on observed pharmacokinetic variables was ruled out using a general linear model analysis of variance for a repeated-measures Latin square experimental design (NCSS 6.0.2 Statistical System for Windows; Number Cruncher Statistical Systems, Kaysville, UT). Some data failed either the Kolmogorov-Smirnov test for a normally distributed population or the Levene median test for equal variance (SigmaStat Statistical Software version 2.0; Jandel Scientific Software, San Rafeal, CA). Therefore, all variables were treated as ordinal data and compared across treatments using the Friedman repeated-measures analysis of variance on ranks. When the analysis of variance met the criterion for rejection of the null hypothesis, *post hoc* comparisons with control were made using

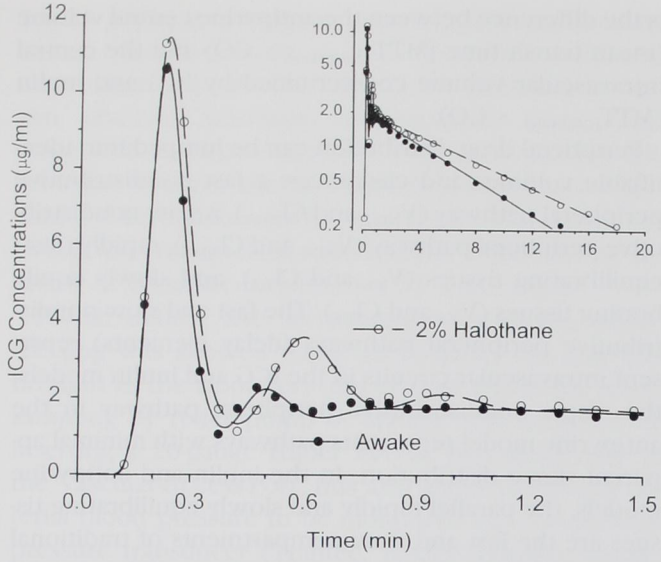

Fig. 2. Arterial blood indocyanine green (ICG) concentration histories for the first 1.5 min (illustrating the first- and second-pass peaks) and for 20 min (inset) after right atrial injection in one dog when it was awake (closed symbols) and when it was anesthetized with 2% halothane (open symbols). The symbols represent drug concentrations and the lines represent concentrations predicted by the models.

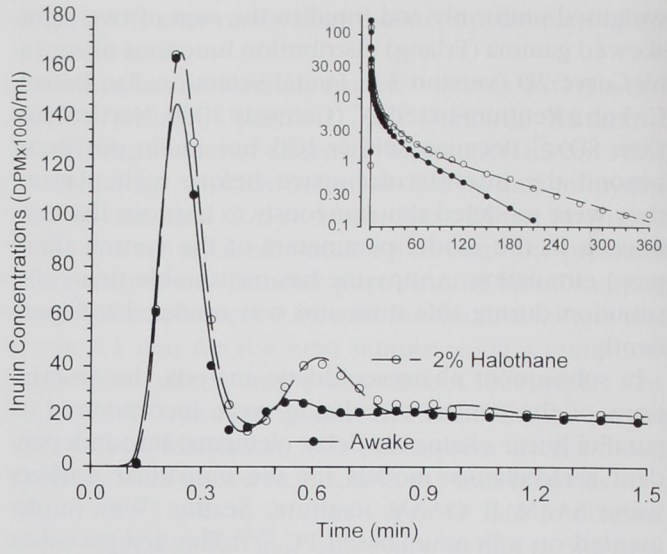

Fig. 3. Arterial blood inulin concentration histories for the first 1.5 min (illustrating the first- and second-pass peaks) and for 360 min, or to the limit of detection (inset), after right atrial injection in one dog when it was awake (closed symbols) and when it was anesthetized with 2% halothane (open symbols). The symbols represent drug concentrations and the lines represent concentrations predicted by the models.

Dunnett's test. The relation of the pharmacokinetic variables to the end-tidal halothane concentration was sought using the Spearman rank-order correlation (SigmaStat) using the Bonferroni correction of the criterion for rejection of the null hypothesis. The criterion for rejection of the null hypothesis was $P < 0.05$.

Results

Halothane anesthesia was associated with a decrease in hematocrit compared with the awake control (table 1). There was a significant, halothane dose-related increase in heart rate and a decrease in blood pressure and CO with no change in systemic vascular resistance.

Global Model Parameters

The blood ICG, inulin, and antipyrine concentration *versus* time relations were well characterized by the models from the moment of injection (figs. 2–4). The one-sample runs test confirmed that there was random scatter of the observed data about the calculated values, indicating that there were no systematic errors produced by the models. Our recirculatory model of drug disposition was able to describe the effect of halothane on CO and its distribution (the ICG model, table 2) and the effect of reduced and

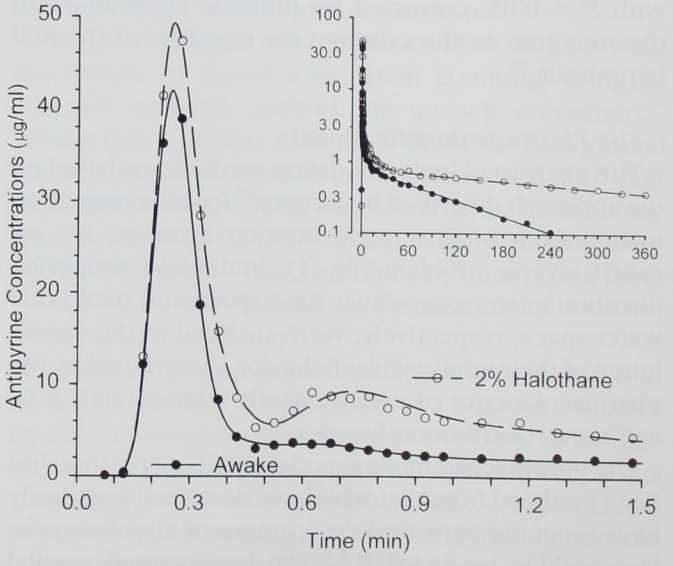

Fig. 4. Arterial blood antipyrine concentration histories for the first 1.5 min (illustrating the first- and second-pass peaks) and for 360 min, or to the limit of detection (inset), after right atrial injection in one dog when it was awake (closed symbols) and when it was anesthetized with 2% halothane (open symbols). The symbols represent drug concentrations and the lines represent concentrations predicted by the models.

Table 2. Pharmacokinetic Variables for Recirculatory Indocyanine Green Kinetic Model

End-tidal Halothane Concentration	Volumes (L)*				Clearances (L/min)†			
	V_C	V_{ND-F}	V_{ND-S}	V_{SS}	Cl_{ND-F}	Cl_{ND-S}‡	Cl_E	ΣCl‡
0% (awake)	0.81	0.26	1.12	2.19	2.16	2.34	0.28	4.77
	(0.14)	(0.23)	(0.24)	(0.48)	(1.17)	(0.24)	(0.11)	(1.33)
1.0%	0.71	0.19	1.20	2.10	1.61	1.51	0.24	3.36§
	(0.14)	(0.05)	(0.41)	(0.52)	(0.33)	(0.28)	(0.08)	(0.33)
1.5%	0.70	0.19	1.30	2.19	1.36	1.54	0.26	3.15§
	(0.09)	(0.04)	(0.26)	(0.25)	(0.53)	(0.48)	(0.09)	(0.46)
2.0%	0.72	0.22	1.21	2.15	1.40	1.00§	0.23	2.62§
	(0.14)	(0.09)	(0.15)	(0.32)	(0.70)	(0.28)	(0.08)	(0.96)

Values are mean (SD).

* The volumes (V) of the central (C), rapidly equilibrating (fast) nondistributive (ND-F), and slowly equilibrating nondistributive (ND-S) intravascular circuits and the volume of distribution at steady-state (V_{SS}), which equals the sum of all volumes.

† The clearance (Cl) of the rapidly (fast) equilibrating nondistributive (ND-F) and slowly equilibrating nondistributive (ND-S) intravascular circuits, elimination clearance (Cl_E), and the sum of all clearances (ΣCl), which equals the ICG (dye dilution) cardiac output determined at the moment of marker injection.

‡ Significantly correlated with end-tidal halothane concentration ($P < 0.05$) as determined by Spearman rank order correlation.

§ Significantly different from awake control ($P < 0.05$) as determined by Dunnett's test.

redistributed CO on inulin (table 3) and antipyrine (table 4) disposition. Our model accounted for the twofold increase in the area under the first minutes of the antipyrine concentration *versus* time curve (AUC) produced by 2% halothane anesthesia (fig. 4, table 5). The total volumes of distribution (V_{SS}) of ICG, inulin, and antipyrine were unaffected by halothane anesthesia (tables 1–4). The ICG Cl_E was not affected by halothane anesthesia (tables 1 and 2; fig. 2 [inset]), but the Cl_E of both inulin and antipyrine were significantly decreased by halothane anesthesia, as reflected in the decreased slopes of their terminal drug concentration *versus* time relations (tables 1, 3, 4; fig. 3 [inset], fig. 4 [inset]).

Indocyanine Green

The volumes of the central and peripheral circulations described by ICG disposition did not change with halothane anesthesia; more than one third of the blood vol-

Table 3. Pharmacokinetic Variables for Recirculatory Inulin Pharmacokinetics

End-Tidal Halothane Concentration	Volumes (L)*						Clearances (L/min)†					
	V_C	V_{ND-F}	V_{ND-S}	V_{T-F}	V_{T-S}	V_{SS}	Cl_{ND-F}	Cl_{ND-S}‡	Cl_{T-F}	Cl_{T-S}	Cl_E‡	ΣCl‡
0% (awake)	0.81	0.15	0.93	2.37	4.82	9.08	1.49	2.32	0.63	0.13	0.20	4.77
	(0.14)	(0.10)	(0.13)	(0.32)	(0.84)	(1.24)	(1.04)	(0.72)	(0.18)	(0.04)	(0.03)	(1.33)
1.0%	0.71	0.19	1.06	2.42	5.35	9.73	1.33	1.33§	0.42	0.13	0.15	3.36§
	(0.14)	(0.03)	(0.39)	(0.48)	(1.46)	(2.42)	(0.24)	(0.31)	(0.03)	(0.04)	(0.02)	(0.33)
1.5%	0.70	0.18	0.93	2.31	5.91	10.03	1.10	1.21§	0.54	0.14	0.15	3.15§
	(0.09)	(0.05)	(0.18)	(0.17)	(1.35)	(1.60)	(0.44)	(0.39)	(0.15)	(0.07)	(0.01)	(0.46)
2.0%	0.72	0.19	1.12	2.14	5.32	9.49	1.17	0.97§	0.27	0.10	0.10§	2.62§
	(0.14)	(0.11)	(0.12)	(0.86)	(1.01)	(2.01)	(0.74)	(0.33)	(0.15)	(0.05)	(0.06)	(0.96)

Values are mean (SD).

* The volumes (V) of the central (C), rapidly equilibrating (fast) nondistributive (ND-F), and slowly equilibrating nondistributive (ND-S) circuits and the rapidly equilibrating (fast) (T-F) and slowly equilibrating (T-S) tissues, and the volume of distribution at steady-state (V_{SS}), which equals the sum of all volumes.

† The clearances (Cl) of the rapidly equilibrating (fast) nondistributive (ND-F) and slowly equilibrating nondistributive (ND-S) circuits and the rapidly equilibrating (fast) (T-F) and slowly equilibrating (T-S) tissues, elimination clearance (Cl_E), and the sum of all clearances (ΣCl), which equals the ICG (dye dilution) cardiac output determined at the moment of marker injection.

‡ Significantly correlated with end-tidal halothane concentration ($P < 0.05$) as determined by Spearman rank order correlation.

§ Significantly different from awake control ($P < 0.05$) as determined by Dunnett's test.

Table 4. Pharmacokinetic Variables for Recirculatory Antipyrine Pharmacokinetics

End-Tidal Halothane Concentration	Volumes (L)*						Clearances (L/min)†				
	V_C	V_{T-P}	V_{ND}‡	V_{T-F}	V_{T-S}	V_{SS}	Cl_{ND}	Cl_{T-F}‡	Cl_{T-S}‡	Cl_E‡	ΣCl‡
0% (awake)	0.89	0.09	0.05	5.18	16.48	22.60	0.33	2.78	1.41	0.247	4.77
	(0.17)	(0.04)	(0.01)	(1.91)	(6.22)	(6.32)	(0.08)	(0.87)	(0.54)	(0.044)	(1.33)
1.0%	0.82	0.10	0.20§	2.20	20.47	23.68	1.12§	1.06§	1.10	0.089§	3.36§
	(0.18)	(0.04)	(0.06)	(1.00)	(7.47)	(7.58)	(0.21)	(0.21)	(0.48)	(0.026)	(0.33)
1.5%	0.81	0.12	0.25§	4.99	19.39	25.44	1.03§	1.40§	0.65§	0.072§	3.15§
	(0.11)	(0.03)	(0.09)	(0.84)	(3.14)	(3.40)	(0.40)	(0.42)	(0.21)	(0.004)	(0.46)
2.0%	0.82	0.10	0.32§	3.58	20.92	25.64	1.24§	0.78§	0.53§	0.061§	2.62§
	(0.14)	(0.02)	(0.09)	(0.80)	(6.09)	(6.90)	(0.71)	(0.30)	(0.18)	(0.010)	(0.96)

Values are mean (SD).

* The volumes (V) of the central (described by ICG and inulin) circuit (C), pulmonary tissue (the difference between the antipyrine central circuit volume and that described by ICG and inulin) (T-P), nondistributive (ND) circuit, and the rapidly equilibrating (fast) (T-F) and slowly equilibrating (T-S) tissues, and the volume of distribution at steady-state (V_{SS}), which equals the sum of all volumes

† The clearances (Cl) of the nondistributive (ND) circuit and rapidly equilibrating (fast) (T-F) and slowly equilibrating (T-S) tissues, elimination clearance (Cl_E), and the sum of all clearances (ΣCl), which equals the ICG (dye dilution) cardiac output determined at the moment of marker injection.

‡ Significantly correlated with end-tidal halothane concentration ($P < 0.05$) as determined by Spearman rank order correlation.

§ Significantly different from awake control ($P < 0.05$) as determined by Dunnett's test.

ume was in the central circuit (V_C), approximately 10% was in the fast nondistributive circuit (V_{ND-F}), and just over half was in the slow nondistributive circuit (V_{ND-S}) (fig. 1, table 2). Halothane did cause a progressive and dose-related decrease in flow through the central circuit (dye-dilution CO), up to a 45% reduction at 2% halothane. The slow nondistributive intercompartmental clearance of ICG (Cl_{ND-S}), but not its fast nondistributive intercompartmental clearance (Cl_{ND-F}), was significantly correlated with end-tidal halothane concentration and was significantly different from the baseline value at 2% end-tidal halothane. The systemic distribution of CO not represented by Cl_E (90–94% of CO) was nearly evenly divided between the peripheral intravascular circuits described by ICG in the awake dog and remained so at 1% and 1.5% halothane anesthesia, with flows through each circuit decreasing directly in proportion to the decrease in CO. At 2% halothane, relatively more of the CO flowed through the fast circuit (51%) than the slow circuit (40%).

Inulin

The volumes of the recirculatory inulin pharmacokinetic model were also unaffected by halothane anesthesia; approximately 20% of the volume of inulin was in the central and peripheral nondistributive circuits,

Table 5. Areas under the Blood Concentrations of the Physiologic Markers *versus* Time Relationships (AUC) for the First min, the First 2 min, and the First 3 min after Right Atrial Injection of Indocyanine Green (ICG), Inulin, and Antipyrine

End-Tidal Halothane Concentration	ICG			Inulin			Antipyrine		
	1 min	2 min	3 min	1 min	2 min	3 min	1 min	2 min*	3 min*
0% (awake)	2.50	4.41	6.10	35.08	55.85	71.80	8.51	10.76	12.74
	(0.52)	(1.04)	(1.53)	(9.66)	(15.64)	(20.39)	(1.18)	(1.59)	(1.95)
1.0%	2.92	4.86†	6.61	39.11†	59.95	76.93	13.51†	17.29†	19.94†
	(0.73)	(1.13)	(1.60)	(9.14)	(12.67)	(16.29)	(1.31)	(1.90)	(2.45)
1.5%	2.83	4.61	6.22	42.71†	64.70	82.54	12.89†	16.63†	19.16†
	(0.41)	(0.59)	(0.87)	(7.41)	(9.72)	(12.74)	(3.74)	(4.45)	(4.75)
2.0%	3.24†	5.14†	6.77	50.10†	76.28	97.57	17.03†	23.32†	27.17†
	(1.02)	(1.26)	(1.46)	(19.59)	(25.96)	(31.22)	(8.95)	(11.33)	(13.16)

Values are mean (SD).

* Significantly correlated with end-tidal halothane concentration ($P < 0.05$) as determined by Spearman rank order correlation.

† Significantly different from awake control ($P < 0.05$) as determined by Dunnett's test.

whereas one quarter of the volume was the rapidly equilibrating (fast) tissue and the balance was the slowly equilibrating tissue (table 3). As in the ICG model, Cl_{ND-S}, but not Cl_{ND-F}, was correlated with end-tidal halothane concentration; in contrast to the ICG model, Cl_{ND-S} was significantly different from the baseline value at all end-tidal halothane concentrations. Approximately 80% of CO was nondistributive in the inulin models in the dogs under all experimental conditions. Although the nondistributive flows were nearly evenly divided between the fast and slow circuits during all levels of halothane anesthesia, in the awake animals 30% was Cl_{ND-F} and nearly 50% was Cl_{ND-S}. Neither the fast nor the slow distributive (intercompartmental, tissue) clearance (Cl_{T-F} and Cl_{T-S}) of inulin was affected by halothane in a statistically significant way in halothane-anesthetized dogs. Inulin Cl_E (glomerular filtration rate) was correlated with end-tidal halothane concentration, and at 2% end-tidal halothane it was significantly less than the baseline value.

Antipyrine

The recirculatory antipyrine pharmacokinetic model was most profoundly affected by halothane anesthesia (table 4). The only peripheral nondistributive volume that could be identified in the antipyrine model, V_{ND},[5] increased significantly and in a halothane dose-related manner from a miniscule volume of 0.05 l in the awake animals to 0.32 l in dogs anesthetized with 2% halothane. The other antipyrine compartmental volumes were largely unaffected by halothane anesthesia; less than 5% of the volume of antipyrine was in the central vascular circuit and pulmonary tissue (V_{T-P}), the latter of which had a volume of approximately 0.1 l. The antipyrine V_{T-F} had approximately 17% of the distribution volume, while the bulk of the volume (79%) was in V_{T-S}. Only 7.5% of CO was nondistributive (Cl_{ND}) in the antipyrine models in awake dogs, but as CO decreased with halothane anesthesia, nondistributive clearance (Cl_{ND}) actually increased significantly, both absolutely and relatively, and represented 33–45% of CO in halothane-anesthetized dogs. Antipyrine tissue distributive clearances (Cl_{T-F} and Cl_{T-S}) not only decreased significantly in absolute terms in a halothane dose-dependent manner but, more importantly, it also decreased as a percentage of CO; although more than 85% of the CO was involved in drug distribution in the awake dogs, this decreased with halothane anesthesia to a minimum at which only 50% of CO was involved in drug distribution in dogs anesthetized with 2% halothane. As a result of the increase in nondistributive clearance and decrease in distributive clearance during halothane anesthesia, the AUC during the first 3 min after drug administration more than doubled (fig. 4, table 5). Antipyrine Cl_E was correlated with end-tidal halothane concentration and was significantly less than the baseline value at all levels of end-tidal halothane.

Discussion

The observed halothane-induced increase in heart rate, decrease in blood pressure, and decrease in CO, with no change in systemic vascular resistance (table 1), is consistent with the cardiovascular effects of halothane reported by others.[1] The association of halothane anesthesia with a decrease in hematocrit has also been described.[31]

Cardiac outputs and halothane dose-related changes in CO determined by ICG and inulin (*i.e.*, indicator) dilution (table 2) are nearly identical to those determined by thermal dilution (table 1), indicating that our sampling schedule was appropriate. These progressive decreases in CO with increasing halothane concentrations are associated with the expected increases in the first-pass AUCs ($AUC_{first\text{-}pass}$ = dose/CO) not only for ICG and inulin but also for antipyrine (figs. 2–4). The first-pass curve is largely complete within the first half minute.

The $AUC_{0-\infty}$ of a complete drug concentration history can also increase significantly as a result of a decrease in the Cl_E of the drug ($AUC_{0-\infty}$ = dose/Cl_E). This Cl_E dependent increase in AUC is readily apparent in the curves of several hours duration, as illustrated in the insets of figures 3 and 4. However, simulations revealed that changes in Cl_E cannot explain the increase in the antipyrine AUC after first-pass, long before Cl_E becomes the major determinant of the drug concentration *versus* time relation (fig. 4).

An important observation of the present study is that halothane anesthesia causes a significant increase in the AUC of antipyrine in the critical first minutes after drug administration due to an increase in the apparent flow of blood not involved in drug distribution to the tissues, despite a halothane dose-dependent decrease in CO. Using the blood drug concentrations of the recirculation (second-pass) peak, the recirculatory model describes an independent nondistributive blood flow, or clearance, which returns the lipophilic marker to the central circulation after minimal tissue equilibration. This pharmacokinetic shunt reflects the inhomogeneity

of tissue blood flow, the presence of significant diffusion barriers, or both. Halothane-induced changes in CO and its distribution alters the balance of distributive and nondistributive blood flows to various tissues, which are not proportional to changes in CO. Because nondistributive blood flow quickly returns the lipophilic marker to the central circulation, the increase in nondistributive blood flow by halothane increases the arterial blood AUC during the early minutes after drug administration (table 5). The increased arterial drug concentrations resulting from a larger nondistributive clearance increases drug exposure of the sites of action of drugs with a rapid onset of effect, for which antipyrine is a pharmacokinetic prototype, and would be expected to result in a more profound and prolonged effect of these drugs.

The study of regional blood flow during halothane anesthesia by Gelman *et al.*[32] suggests the basis of the increase in nondistributive blood flow during halothane anesthesia in dogs. These investigators found that during 1 and 2 minimum alveolar concentration halothane anesthesia, the percentage shunting of 15-μm radiolabeled microspheres was 2.5 and 4 times that during awake control, respectively. Although preportal and muscle blood flow decreased in these studies, renal blood flow was preserved and cerebral blood flow nearly doubled. Thus the substantial increase in nondistributive blood flow described in the present recirculatory antipyrine pharmacokinetic model may be due, at least in part, to the decrease in muscle tissue blood flow and the maintenance of renal blood flow (which is essentially nondistributive) described by Gelman *et al.*[32] Together, the doubling of the antipyrine $AUC_{0-3\ min}$ due to increased nondistributive blood flow observed in the present study and the near doubling of cerebral blood flow reported by Gelman *et al.*[32] would provide mechanistic explanations for profound increases in the central effects of intravenous anesthetic agents administered during halothane anesthesia.

Physiologically based pharmacokinetic models describe measured blood and tissue drug concentration histories by proportioning CO, and hence drug distribution, among tissues or tissue groups with similar perfusion and drug solubility characteristics.[39] These models have proved useful in providing insight into factors affecting drug disposition[33] and predicting the effect of altered physiology on drug disposition.[34] However, such models have well-known limitations, including their requirements for large amounts of data (tissue drug concentrations and blood flows), which are often unavailable (especially in humans), their inability to characterize individuals, and their many assumptions that ignore interindividual variability and physiologic changes.[39] They are also limited by the many assumptions that must be made in interpreting tissue concentration data and adjusting the model for different conditions of body composition and blood flow. For example, because physiologic models generally assume that tissue blood flow is homogeneous, some models assume all blood leaving a tissue is in equilibrium with it,[34] whereas others interpret their tissue data as demonstrating diffusion barriers for flow-limited drug uptake.[35] When simulating drug disposition in the presence of altered physiology, physiologic models adjust regional blood flows in one of several ways. Regional blood flows may be changed in physiologic simulations in direct proportion to changes in CO,[36] or adjusted arbitrarily and independently,[34] or adjusted based on radioactive microsphere regional blood flow measurements[37,38] while maintaining the assumption of either complete tissue equilibration with exiting blood or diffusion barriers for flow-limited drug uptake.

Traditional multicompartmental pharmacokinetic models are mathematical constructs based on the characterization of the multiexponential plasma drug concentration *versus* time relation.[39] These models have been useful in characterizing drug disposition in subjects under various conditions and provide guidance for drug dosing, particularly when drugs are administered as multiple doses or by continuous infusion. However, because these models lack an anatomic and physiologic basis, they cannot be used to predict the effect of alterations in CO on drug disposition. In addition, neither the traditional compartmental model nor the physiologic model account for measured drug blood, or tissue, concentrations in the first minutes after drug administration when intravenous anesthetic drugs produce their maximum effect.[40]

The present recirculatory multicompartmental model of the disposition of physiologic markers based on frequent early arterial blood sampling retains the best aspects of the traditional multicompartmental model and the physiologically based model besides offering several significant advantages over both. The traditional multicompartmental model and the recirculatory model describe data from individuals (including humans) collected under various conditions, such as physiologic changes produced by different levels of anesthesia. The physiologic model and the recirculatory model incorporate physiologic factors, such as CO and its distribution, in a description of drug disposition. However, only the

recirculatory model can describe drug disposition from the moment of injection, including a description of pulmonary drug distribution (uptake), which an early version of this model[41] lacked.[42] Unlike the physiologic models, a recirculatory model neither assumes that all tissues are in equilibrium with the blood leaving it nor invokes the concept of diffusion barriers for flow-limited drug uptake. Instead, the recirculatory model uses the blood drug concentrations of the recirculatory peak to describe a nondistributive blood flow, or clearance, which returns blood to the central circulation after minimal tissues equilibration. This can be thought of as a pharmacokinetic shunt (second-pass peak, figs. 1–4).

The AUC is often used as a measure of drug exposure. In evaluating the effect of changes in AUC, the time course of drug effect must be considered. For example, the $AUC_{0-\infty}$ for cancer chemotherapeutic agents has been correlated with efficacy and toxicity because these drugs, which act irreversibly, produce effects that are a function of the product of drug concentration and time.[43] For rapidly and reversibly acting drugs, it may be more useful to gauge drug exposure of the effector site by arterial AUC during times that might correspond to peak drug effect.

The increase in AUC of antipyrine for at least the first 3 min after drug administration is due to increased nondistributive blood flow during halothane anesthesia (table 5) and reflects an increased exposure of the brain to antipyrine. For rapidly acting drugs, such as the centrally acting intravenous anesthetics for which the lipophilic marker antipyrine is a prototype, this increase in nondistributive blood flow (and, as a result, AUC) would produce a more profound and longer-lasting drug effect due to exposure of potential sites of drug action to higher drug concentrations for a longer period of time. A more profound onset and longer duration of effect of the hydrophilic drugs for which inulin is a prototype (*e.g.*, the relatively slow-onset neuromuscular blockers) is not likely to be seen during halothane anesthesia for distributional pharmacokinetic reasons because observed differences in the AUC of inulin did not correspond to the expected time course of drug (*e.g.*, neuromuscular blocker) onset and duration of action (table 5).

Appendix

Traditional three-compartment pharmacokinetic models are constructed from triexponential equations describing the blood or plasma drug concentration *versus* time relation. The initial volume of distribution (V_I) is that volume in which a drug appears to mix instantaneously before being distributed throughout the rest of the total volume of distribution; the volume estimate of V_I is related to the time interval between drug administration and the collection of the first blood samples, because the drug will be more extensively distributed with the passage of time. From V_I, drug distributes throughout the rest of its volume by a process called intercompartmental clearance (Cl_I) and is irreversibly removed from the body by elimination clearance (Cl_E). The volume of distribution at steady state (V_{SS}) is the total volume of distribution and, as such, is the sum of V_I and the rapidly (fast) and slowly equilibrating volumes of distribution (V_F and V_S, respectively). Intercompartmental clearances between V_I and both V_F and V_S (Cl_F and Cl_S, respectively) are volume-independent estimates of drug transfer that are directly determined by blood flow and transcapillary permeability.

The recirculatory pharmacokinetic model of ICG disposition based on frequent early arterial blood samples describes intravascular mixing and blood flows through the many circuits of the body by deriving estimates of not only blood volume and CO but also their systemic distribution (fig. 1). The many blood circuits lump into kinetically distinct pathways based on their blood volume to blood flow ratios (MTTs).[5,9,44,45] This ICG pharmacokinetic model is isomorphic with the lumped parameter recirculatory models describing the physiology of the systemic circulation,[46–48] which have a central volume and two parallel peripheral circuits representing the peripheral circulation. These parallel peripheral circulations are characterized by time constants that reflect a low capacitance, low volume (fast) circuit and a high capacitance, larger volume (slow) circuit, the latter of which presumably represents the splanchnic circulation. Both the physiologic models and our model distribute CO between the two parallel peripheral circuits, and the models can accommodate the redistribution of CO and blood volume. Physiologic models require estimates of blood flow to each significant tissue group. Recirculatory models contain estimates of the lumped behavior of the circulation, which are determined directly from easily acquired data. This multicompartmental recirculatory model can be interpreted physiologically.[49]

Simultaneous time-density function analysis of an intravascular marker and a tissue water marker has been used to estimate extravascular lung water.[50,51] Blood flow to the lungs is assumed to be the CO determined by ICG and inulin kinetics, and the central (thoracic) blood volume is derived from the product of CO and the MTT for the markers between the injection and sampling sites. Similarly, the antipyrine central volume is the product of the composite mean transit time of the central pathways for antipyrine and the CO.[8] The apparent lung tissue volume ($V_{T\text{-}P}$) of antipyrine is the difference between the antipyrine central blood and tissue volume and central intravascular volume codetermined by ICG and inulin.

Characterization of the dispositions of inulin and antipyrine simultaneously with that of ICG allows characterization of their early disposition as the convolution of their intravascular behavior, determined by the pharmacokinetics of concomitantly administered ICG and tissue distribution pharmacokinetics.[5] For pharmacokinetic models in which drug distribution is known to occur from intravascular space, defined in the present recirculatory models, Cl_I occurs by transcapillary exchange, which is determined by blood flow (Q) and diffusion (capillary permeability coefficient surface area product, P)[52,53]:

$$Cl_I = Q\,(1 - e^{-P/Q}) \qquad (1)$$

The physicochemical properties of some substances, such as antipyrine, make them freely diffusible; for them, Cl_I approaches actual

blood flow to tissue (*i.e.*, $Cl_I = Q$ when $P \gg Q$ because $e^{-P/Q} \rightarrow 0$).[52,53] For substances that are not freely diffusible, such as inulin, Cl_I is related to the permeability coefficient surface area product (*i.e.*, $Cl_I = P$ when $P \ll Q$ because the higher-order terms of the series expansion of equation 1 can be neglected).[52,53] The difference between CO and the sum of intercompartmental clearance to tissues for a given drug is the portion of CO not involved in flow-limited tissue distribution of that drug, or nondistributive flow, which returns (shunts) drug to the central circuit. Tissue volume to tissue distribution clearance ratios determine whether a compartment is a fast or slow nondistributive peripheral pathway or a rapidly or slowly equilibrating tissue.[5,45]

Our model also includes recirculation and time delays, as does the detailed model of the circulation developed by Jacquez *et al.*[54] A time delay accounts for the noninstantaneous appearance of drugs in a compartment after being transferred from another compartment. A delay element is a mathematical description of the distribution of drug transit times which can be described by the average (MTT). It also has an associated apparent volume calculated as the product of the flow through the delay and its MTT. In the recirculatory model, the central delay represents the central blood and tissue volume between the sites of drug injection and blood sampling. The peripheral delay elements represent kinetically distinct peripheral nondistributive pathways. Because flow in a medium generates a distribution of time lags,[29] the time delays in the present model are represented as delay elements rather than as discrete time lags, which are more appropriate for characterizing ideal plug flow models.

We used the distributed delay elements of the SAAM II kinetic analysis software to describe the first-pass data in the recirculatory model.[25] These delay elements are composed of n compartments connected by identical rate constants k such that n/k is equal to the MTT for the delay. As n increases, the arterial drug appearance curve becomes narrower until at $n = \infty$ the delay becomes a discrete lag (*i.e.*, a spike). Normally the number of compartments, n, in a model cannot be adjusted during parameter optimization. Therefore, we fit the first-pass data using the closed form equations of this type of distributed delay in sequence and the TableCurve 2D software. First, the data, weighted uniformly, were fit to the sum of two gamma distribution functions, which allow n to be any positive value (*i.e.*, it permits fractional compartments). Then n was rounded to the nearest integer value and fixed as a constant, and the data were fitted again using the sum of two Erlang distribution functions; the Erlang function is essentially the gamma distribution with n confined to integer values (*i.e.*, it permits only whole compartments):

$$C(t) = A_1 \cdot \frac{k_1^{n_1} \cdot t^{n_1-1}}{(n_1 - 1)!} \cdot e^{-k_1 t} + A_2 \cdot \frac{k_2^{n_2} \cdot t^{n_2-1}}{(n_2 - 1)!} \cdot e^{-k_2 t} \qquad (2)$$

where A_1 and A_2 are the proportional blood flows through the two parallel elements. Thus the number of compartments for the delay element, their rate constants, CO (ICG and inulin), and the proportion of flow through each parallel central pathway are estimated. These results were placed as fixed parameters into the recirculatory model.

The central circuits and the nondistributive peripheral compartments (shunts) can be estimated only by obtaining frequent early arterial blood samples. If a less-rigorous sampling schedule is used (*i.e.*, if the sampling frequency is inadequate to define the first- and second-passes), then these data can only be modeled as the traditional V_1. V_F and V_S so derived are similar (equivalent) to the peripheral tissue compartments in the recirculatory model.

The authors thank Mary Pat Janowski for technical assistance.

References

1. Pagel PS, Kampine JP, Schmeling WT, Warltier DC: Comparison of the systemic and coronary hemodynamic actions of desflurane, isoflurane, halothane, and enflurane in the chronically instrumented dog. ANESTHESIOLOGY 1991; 74:539–51

2. Runciman WB, Myburgh JA, Upton RN, Mather LE: Effects of anaesthesia on drug disposition, Mechanisms of Drugs in Anaesthesia. Edited by S Feldman, CF Scurr, W Paton. Boston, Edward Arnold, 1993, pp 93–128

3. Sheiner LB, Benet LZ, Pagliaro LA: A standard approach to compiling clinical pharmacokinetic data. J Pharmacokin Biopharm 1981; 9:59–127

4. Riggs DS: The Mathematical Approach to Physiological Problems: A Critical Primer. Cambridge, MA, MIT Press, 1963

5. Krejcie TC, Henthorn TK, Niemann CU, Klein C, Gupta DK, Gentry WB, Shanks CA, Avram MJ: Recirculatory pharmacokinetic models of markers of blood, extracellular fluid and total body water administered concomitantly. J Pharmacol Exp Ther 1996; 278:1050–7

6. Cherrick GR, Stein SW, Leevy CM, Davidson CS: Indocyanine green: Observations on its physical properties, plasma decay, and hepatic extraction. J Clin Invest 1960; 39:592–600

7. Bradley EC, Barr JW: Determination of blood volume using indocyanine green (Cardio-Green®) dye. Life Sci 1968; 7:1001–7

8. Zierler KL: Circulation times and the theory of indicator-dilution methods for determining blood flow and volume, Handbook of Physiology, section 2, Circulation, vol. 1. Edited by WF Hamilton. Washington, DC, American Physiological Society, 1962, pp 585–615

9. Henthorn TK, Avram MJ, Krejcie TC, Shanks CA, Asada A, Kaczynski DA: Minimal compartmental model of circulatory mixing of indocyanine green. Am J Physiol 1992; 262:H903–10

10. Wilkinson GR, Shand DG: A physiological approach to hepatic drug clearance. Clin Pharmacol Ther 1975; 18:377–90

11. Ketterer SG, Wiegand BD, Rapaport E: Hepatic uptake and biliary excretion of indocyanine green and its use in estimation of hepatic blood flow in dogs. Am J Physiol 1960; 199:481–4

12. Henthorn TK, Avram MJ, Frederiksen MC, Atkinson AJ Jr: Heterogeneity of interstitial fluid space demonstrated by simultaneous kinetic analysis of the distribution and elimination of inulin and gallamine. J Pharmacol Exp Ther 1982; 222:389–94

13. Holstein-Rathou N-H, Christensen P, Leyssac PP: Effects of halothane-nitrous oxide inhalation anaesthesia and inactin on overall renal and tubular function in Sprague-Dawley and Wistar rats. Acta Physiol Scand 1982; 114:193–201

14. Soberman R, Brodie BB, Levy BB, Axelrod J, Hollander V, Steele JM: The use of antipyrine in the measurement of total body water in man. J Biol Chem 1949; 179:31–42

15. Brigham KL, Ramsey LH, Snell JD, Merritt CR: On defining the pulmonary extravascular water volume. Circ Res 1971; 29:385–97

16. Renkin EM: Capillary permeability to lipid-soluble molecules. Am J Physiol 1952; 168:538–45

17. Krejcie TC, Henthorn TK, Shanks CA, Avram MJ: A recircula-

tory pharmacokinetic model describing the circulatory mixing, tissue distribution, and elimination of antipyrine in dogs. J Pharmacol Exp Ther 1994; 269:609–16

18. Vessel ES: The antipyrine test in clinical pharmacology: Conceptions and misconceptions. Clin Pharmacol Ther 1979; 26:275–86

19. Cousins MJ, Gourlay GK, Knights KM, de la Hall P, Lunam CA, O'Brien P: A randomized prospective controlled study of the metabolism and hepatotoxicity of halothane in humans. Anesth Analg 1987; 66:299–308

20. Garner D, Laks MM: New implanted chronic catheter device for determining blood pressure and cardiac output in conscious dogs. Am J Physiol 1985; 249:H681–4

21. Eger EI: Anesthetic Uptake and Action. Baltimore, Williams and Wilkins, 1974

22. Atlee JL III, Brownlee SW, Burstrom RE: Conscious-state comparisons of the effects of inhalation anesthetics on specialized atrioventricular conduction times in dogs. ANESTHESIOLOGY 1986; 64:703–10

23. Grasela DM, Rocci ML Jr, Vlasses PH: Experimental impact of assay-dependent differences in plasma indocyanine green concentration determinations. J Pharmacokin Biopharm 1987; 15:601–13

24. Bowsher DJ, Krejcie TC, Avram MJ, Chow MJ, del Greco F, Atkinson AJ Jr: Reduction in slow intercompartmental clearance of urea during dialysis. J Lab Clin Med 1985; 105:489–97

25. Krejcie TC, Jacquez JA, Avram MJ, Niemann CU, Shanks CA, Henthorn TK: Use of parallel Erlang density functions to analyze first-pass pulmonary uptake of multiple indicators in dogs. J Pharmacokin Biopharm 1996; 24:569–88

26. Krejcie TC, Avram MJ, Gentry WB, Niemann CU, Janowski MP, Henthorn TK: A recirculatory model of the pulmonary uptake and pharmacokinetics of lidocaine based on analysis of arterial and mixed venous data from dogs. J Pharmacokin Biopharm 1997; 25:69–90

27. Berman M, Shahn E, Weiss MJ: The routine fitting of kinetic data to models: A mathematical formalism for digital computers. Biophysical J 1962; 2:275–87

28. Siegel S: Nonparametric Statistics for the Behavioral Sciences. New York, McGraw-Hill, 1956

29. Jacquez JA: Compartmental Analysis in Biology and Medicine, 3rd ed. Ann Arbor, BioMedware, 1996

30. Jacquez JA, Perry TJ: Parameter estimation: Local identifiability of parameters. Am J Physiol 1990; 258:E727–36

31. Albert SN: Blood Volume and Extracellular Fluid Volume. Springfield, IL, Charles C Thomas, 1971

32. Gelman S, Fowler KC, Smith LR: Regional blood flow during isoflurane and halothane anesthesia. Anesth Analg 1984; 63:557–65

33. Price HL, Kovnat PJ, Safer JN, Conner EH, Price ML: The uptake of thiopental by body tissues and its relation to the duration of narcosis. Clin Pharmacol Ther 1960; 1:16–22

34. Price HL: A dynamic concept of the distribution of thiopental in the human body. ANESTHESIOLOGY 1960; 21:40–5

35. Ebling WF, Wada DR, Stanski DR: From piecewise to full physiologic pharmacokinetic modeling: Applied to thiopental disposition in the rat. J Pharmacokin Biopharm 1994; 22:259–92

36. Davis NR, Mapleson WW: A physiological model for the distribution of injected agents, with special reference to pethidine. Br J Anaesth 1993; 70:248–58

37. Benowitz N, Forsyth RP, Melmon KL, Rowland M: Lidocaine disposition kinetics in monkey and man: I. Prediction by a perfusion model. Clin Pharmacol Ther 1977; 16:87–98

38. Benowitz N, Forsyth RP, Melmon KL, Rowland M: Lidocaine disposition kinetics in monkey and man: II. Effects of hemorrhage and sympathomimetic drug administration. Clin Pharmacol Ther 1977; 16:99–109

39. Stanski DR: Pharmacokinetic modelling of thiopental. ANESTHESIOLOGY 1981; 54:446–8

40. Sear JW: Why not model physiologically? Br J Anaesth 1993; 70:243–5

41. Avram MJ, Krejcie TC, Henthorn TK: The relationship of age to the pharmacokinetics of early drug distribution: The concurrent disposition of thiopental and indocyanine green. ANESTHESIOLOGY 1990; 72:403–11

42. Hull CJ: How far can we go with compartmental models? ANESTHESIOLOGY 1990; 72:399–402

43. Powis G: Anticancer drug pharmacodynamics. Cancer Chemother Pharmacol 1985; 14:177–83

44. Hoeft A, Schorn B, Weyland A, Scholz M, Buhre W, Stepanek E, Allen SJ, Sonntag H: Bedside assessment of intravascular volume status in patients undergoing coronary bypass surgery. ANESTHESIOLOGY 1994; 81:76–86

45. Weiss M, Roberts MS: Tissue distribution kinetics as determinant of transit time dispersion of drugs in organs: Application of a stochastic model to the rat hindlimb. J Pharmacokin Biopharm 1996; 24:173–96

46. Caldini P, Permutt S, Waddell RA, Riley RL: Effect of epinephrine on pressure, flow, and volume relationships in the systemic circulation of dogs. Circ Res 1974; 34:606–23

47. Coleman TG, Manning RD Jr, Norman RA Jr, Guyton AC: Control of cardiac output by regional blood flow distribution. Ann Biomed Eng 1974; 2:149–63

48. White RJ, Fitzjerrell DG, Croston RC: Fundamentals of lumped compartmental modelling of the cardiovascular system, Advances in Cardiovascular Physics, vol. 5, Cardiovascular Engineering Part I: Modelling. Edited by DN Ghista, E. Van Vallenhoven, W-J Yang, H Reul, W Bleifeld. New York, Karger, 1983, pp 162–84

49. DiStefano JJ III, Landaw FM: Multiexponential, multicompartmental, and noncompartmental modeling. I. Methodological limitations and physiological interpretations. Am J Physiol 1984; 246:R651–64

50. Brigham KL, Ramsey LH, Snell JD, Merritt CR: On defining the pulmonary extravascular water volume. Circ Res 1971; 29:385–97

51. Effros RM, Mason GR, Reid E, Graham L, Silverman P: Diffusion of labeled water and lipophilic solutes in the lung. Microvasc Res 1985; 29:45–55

52. Renkin EM: Effects of blood flow on diffusion kinetics in isolated perfused hindlegs of cats: A double circulation hypothesis. Am J Physiol 1955; 183:125–36

53. Stec GP, Atkinson AJ Jr: Analysis of the contributions of permeability and flow to intercompartmental clearance. J Pharmacokin Biopharm 1981; 9:167–80

54. Jacquez JA, Bellman R, Kalaba R: Some mathematical aspects of chemotherapy. Bull Math Biophys 1960; 22:309–22